IJEMD-CSAI, 2 (1) (2023), 1 –15 https://doi.org/10.54938/ijemdcsai.2023.02.1.239
International Journal of Emerging Multidisciplinaries:
Computer Science and Artificial Intelligence

Research Paper
Journal Homepage: www.ojs.ijemd.com
ISSN (print): 2791-0164 ISSN (online): 2957-5036

An Intracranial Tumor Detection using Magnetic Resonance Imaging and Deep Learning

Sibtain Syed[1*], Maqbool Khan[1], Rehan Ahmed[1] and Syed Muhammad Talha[2]

[1] Department of IT & CS, Pak-Austria Fachhochschule institute of Applied Sciences and Technology (PAF-IAST), Haripur, Pakistan
[2] National University for Science and Technology (NUST), Islamabad, Pakistan
**Corresponding author*

Abstract

An Intracranial tumor is a malignant CNS cancer, and early prediction can boost patient survival rates. Magnetic Resonance Imagining (MRI) has emerged as an effective non-invasive way to extract 2D or 3D images of human internal organs, eliminating any pain or surgical procedures. Distinguishing normal from abnormal tissue imagery is a challenging task. Yet data-driven models can efficiently classify and detect tumor malignancy. The aim of this study is to efficiently predict Brain tumors by employing sophisticated optimized Deep learning models like CNN and LSTM through limited MRI images dataset of human brain. 253 MRI images dataset acquired from Kaggle covering different angles of the human brain was used. Images of varied sizes and shapes were standardized through data preprocessing, involving resizing and normalizing. One Hot Encoding was used to convert the images to a binary format (0,1) for improved categorization. A 90:10 training-to-testing data ratio was employed. Optimal hyperparameters for the CNN and LSTM models were determined through a trial-and-error approach to enhance model performance on the training data. Model Evaluation by confusion matrix revealed average accuracy, specificity, recall, and misclassification error of 91.51, 92.85, 90.12, and 8.49 for CNN, and 95.54, 92.86, 94.2, and 5.805 for LSTM model.

Keywords: Brain Tumor Detection; Classification; Convolutional Neural Network; Deep learning; Long-Short Term Memory.

1. Introduction

Human brain is a complex organ that functions as a central processing unit of the nervous system. Its primary role involves the regulation and coordination of various physiological processes and behaviors such as respiratory rate, cardiac activity, and thermoregulation. The brain is comprised of an extensive network of neurons, numbering billions that communicate through intricate patterns of electrical and chemical signaling. Numerous disorders affect the brain, one of which is brain tumors. This condition is characterized by the emergence of an abnormal mass or growth within the brain or adjacent tissues. Brain

Email addresses: sibtainshah621@gmail.com (S. Syed), Maqbool.khan@scch.at (M. Khan), rehanahmedahmed007@gmail.com (R. Ahmed), muhammadtalha301@hotmail.com (SM. Talha)

tumors can be benign (non-cancerous) or malignant (cancerous). They can originate within the brain (primary brain tumor) or metastasize to the brain from other parts of the body (metastatic brain tumor). It was estimated that 24,530 adults in the United States will receive a diagnosis of primary malignant brain tumors in 2021, comprising 13,480 males and 10,690 females [1]. Brain tumors make up 85% to 90% of primary nervous system tumors. The survival rates are affected by factors such as age, gender, and tumor type.

As medical technology advances, the usage of crucial medical data for monitoring, prevention, and diagnosis of infectious tumors upsurges. This process usually depends upon managing, collecting, and analyzing the data set for infectious tumor diagnosis and treatment [2, 3, 4]. The timely detection of a brain tumor can have a positive impact on the patient's chances of survival and quality of life. As a result, the implementation of accurate techniques for the detection and classification of brain tumors has become an area of significant interest in recent years [5–7]. Brain tumor detection by using medical imaging commonly involves the analysis of a sequence of image slices within a scan such as Magnetic Resonance Imagining (MRI) and Computed Tomography (CT) scan. MRI scans are capable of illustrating both 2D and 3D images of a human's internal organs non-invasively and without causing any pain or requiring surgical intervention [8]. It is known to be an accurate method for the early detection and diagnosis of human cancer.

However, accurately labeling each slice is recognized as a laborious process that requires considerable expertise and experience and is susceptible to errors. Detecting brain tumors through medical imaginrequires the acquisition of imaging data from various angles, given that tumors can develop in different regions of the brain and exhibit various sizes and shapes. Therefore, a significant data set is required to cover all the possible aspects for future classification.

Brain tumors detection poses a challenge due to the difficulty in distinguishing abnormal tissues from normal ones. A timely diagnosis of brain tumors facilitates rapid patient recovery from treatment. Despite substantial research efforts, the identification of brain tumors continues to face certain limitations attributed to the atypical distribution pattern of the malignancies. Due to their similarity to healthy tissue in small areas, locating regions harboring a limited number of lesions can be challenging. On the other hand, the availability of publicly accessible data sets for brain tumor research is limited due to the concerns of patient confidentiality. The proposed study also addresses this lack of data limitation by using advanced deep learning algorithms like Convolutional Neural Networks (CNN) and Long-Short Term Memory (LSTM). These algorithms provide high accuracy on image data due to their ability to identify patterns and learn distinctive features from the input images through repeated convolutions, leading to highly effective feature extraction capabilities.

The present study is arranged into several sections, starting with similar work to respective study in the following section 2. Subsequently, section 3, represents an overview of the classifiers used in the following study. Section 4 explains the proposed methodology, while section 5 explores the consequential findings and insights. Finally, section 6 provides the concluding remarks of the paper.

2. Related Work

Most of the recent studies have accommodated these shortcomings by applying various deep learning algorithms and image segmentation [9, 10]. An experiment was made by Masoumeh Siar et. al, which concluded that CNN has obtained more significant results than other machine learning algorithms in classifying brain tumors from MRI images [11]. Another study was done by Tonmoy Hossain et al. which concluded that CNN outperformed other machine learning algorithms [12]. In 2022, Wenhao lai and his team concluded that L-Masked R-CNN outperformed U-NET, YOLO v4, Center Net, and Deep Lab v3+ in predicting 2D-shaped gangue [13]. Also, R. Ezhilarasi et. al proposed a system that uses the AlexNet model for classifying and Region Proposal Network by Faster R-CNN for predicting regions of different types of tumors [14]. In 2022, Alanazi and his team re-utilized isolated-CNN model through transfer learning for classifying brain tumor through MRI images [8].

Although these approaches have produced favorable outcomes, they impose high computational costs that are not practical for use on most IOT devices. Saeedi et al. (2023) compared applied machine learning techniques; the study has concluded that K-Nearest Neighbor (KNN) performs robustly from Multilayer Perceptron (MLP) with 86% accuracy [15]. Shanti et al (2022) also applies CNN-LSTM on MRI base brain tumor dataset which resulted in achieving 97.5% accuracy [16]. In 2021, Kumar et al. also imposed adaptive k-nearest neighbor (KNN) for classifying tumor images as normal or abnormal while the regions were segmented by possibilistic fuzzy C-means clustering algorithm [17]. Zhou et. al performed radiomics model by automated machine learning (AutoML) with Tree-Based Pipeline Optimization Tool [18].

The primary objective of the proposed study is to devise an optimized data-driven model tailored explicitly for tumor detection. The research endeavors to overcome the challenge of training such a model with a limited number of tumor images. By leveraging state-of-the-art techniques in machine learning and data analysis, the goal is to craft an algorithm that demonstrates exceptional accuracy and sensitivity in identifying tumors within medical imaging data. The study aims to employ innovative methodologies, such as data formatting, data preprocessing, and hyper-parameter tuning to maximize the model's efficacy despite the scarcity of training data. Successfully developing a model with high detection accuracy using a reduced dataset has the potential to revolutionize medical imaging technologies, enabling more accessible and efficient tools for early tumor detection, thereby significantly impacting patient care and healthcare practices.

Table 1: Literature's Related Work for the respective study

Ref.	Year	Technique	Evaluation Metrics	Data
[19]	2021	16-layer VGG-16 deep NN	Accuracy = 98%	Hospitals' dataset from 2010–2015, China
[20]	2023	Fine-Tuned CNN with ResNet50 and U-Net Model	IoU = 0.91 DSC = 0.95 SI = 0.95	Dataset of TCGA-LGG and TCIA
[21]	2019	pre-trained GoogLeNet	Accuracy = 98% AUC, precision, recall, F-score and specificity	MRI dataset from figshare.
[22]	2022	RCNN-based model	Accuracy = 98.21%	Datasets from Figshare
[23]	2019	CNN implied on Segmented Lesion Images	Accuracy = 98.93% Sensitivity = 98.2%	Dataset of 3064 T1 weighted contrast-enhanced
[24]	2022	Hybrid CNN-SVM	Accuracy = 98.49%	BRATS 2015
[25]	2022	k-NN and SVM classifiers	Accuracy = 97.25%	Figshare, 2017
[26]	2022	ImageNet-based ViT	Accuracy = 98.7%	Figshare
[27]	2021	Hybrid deep learning-based	Accuracy = 96%	ISLES2015 and BRATS2015
[28]	2020	Kernel-based SVM	Accuracy = 97%	Figshare
-	Proposed 2023	Optimized CNN and LSTM model classification for limited data.	CNN acc. = 97.3% LSTM acc.= 98.2% Specificity misclassification error Recall	Kaggles Dataset

Table 1 shows the past studies made relevant to the proposed study and compares them with each other. The proposed study is made on a different dataset with different model evaluation metrics to analyze the results.

3. Models

3.1 Convolution Neural Networks (CNN)

A CNN is a type of neural network architecture commonly used in deep learning for image recognition, object detection, and other visual tasks. In a CNN, the input image is passed through a series of convolutional layers, where each layer applies a set of filters to the input image, extracting features from it. The mathematical output size for these Convolutional layers is shown in equation 1 [29].

$$O = 1 + \frac{i - f}{s} \tag{1}$$

The disadvantage of convolution step is the possible loss of detail at the edges of an image as the output for 6×6 image will be 4×4 image. By using zero-padding this problem is resolved. The equation of output after applying zero-padding will be as in equation 2 [29].

$$O = 1 + \frac{i + 2z - f}{s} \tag{2}$$

Where O is the output size, while i, f, and s represent the input size, filter size and stride size, respectively. While z is the number of zero-padding layers.

These features are then passed through pooling layers, which down-sample the features and reduce the dimensionality of the output. The resulting features are typically passed through flattened layer where they are transformed into one-dimensional (1D) array of vectors (or number). Then they are fed into one or more fully connected layers (also known as dense layers), which perform classification or regression tasks.

CNNs have been particularly successful in computer vision tasks such as image classification, object detection, and segmentation. They have also been used in natural language processing and speech recognition tasks. The working of CNN can be seen in Figure 1.

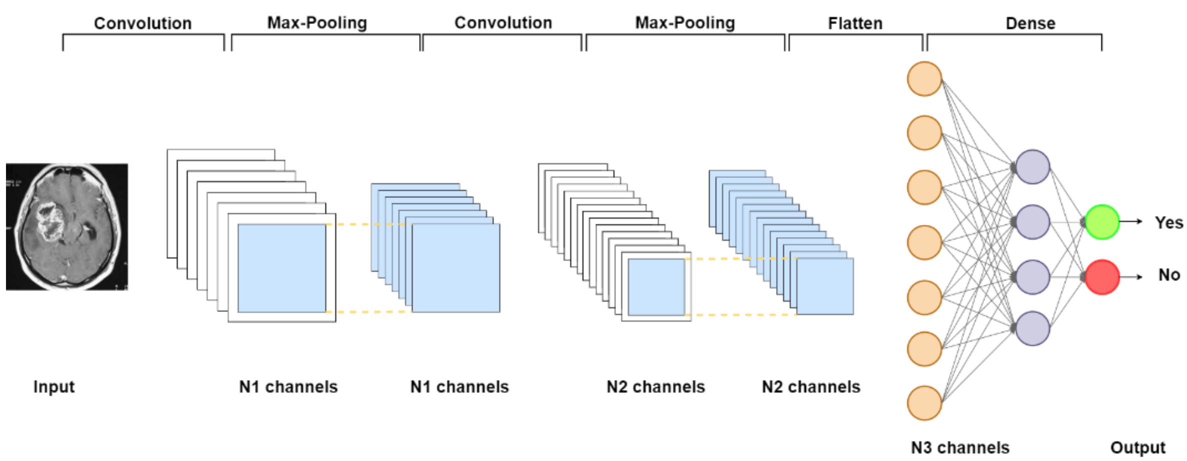

Fig. 1. *Graphical Representation of Convolution Neural Network*

3.2 Long Short-Term Memory (LSTM)

A Long Short-Term Memory (LSTM) is a type of Recurrent Neural Network (RNN) designed to handle sequential data by effectively capturing and retaining long-term dependencies. LSTM networks can excel at handling sequential data, such as sequences of medical images from MRI scans. They are particularly useful for capturing long-term dependencies and temporal patterns in the data, which can be critical for identifying tumors or abnormalities that may not be immediately apparent in individual images. LSTMs can work in conjunction with Convolutional Neural Networks (CNNs) to combine spatial and temporal information effectively. They are also capable of generating synthetic data for data augmentation, helping to address limited training data. While not the sole solution, LSTMs play a valuable role in enhancing the accuracy of brain tumor classification models.

An LSTM model is comprised of memory cells with components such as input gate (Vinput), Forget gate (Vforget), Control gate (Vcontrol), and output gate (Voutput) which are mathematically expressed as following equations [30].

$$V_{input} = \sigma(w_i \times |h_{t-1}, x_t| + b_i) \quad (3)$$

The input gate is defined by equation 3, which determines the transferability of information from a recent cell to the present cell.

$$V_{forget} = \sigma(w_f \times |h_{t-1}, x_t| + b_f) \quad (4)$$

The forget gate is defined by equation 4, in which the previous memory of the input is stored.

$$V_{control} = V_{forget} \times c_{t-1} + V_{input} * c_t) \quad (5)$$

The control gate is defined by equation 5, which modifies the cell.

$$V_{output} = \sigma(w_c \times |h_{t-1}, x_t| + b_o) \quad (6)$$

The output gate is defined by equation 6, indicating the next hidden state.

$$h_t = V_{output} \times tanh\,(c_t) \quad (7)$$

Where w represents the weight of the corresponding matrix while b denotes the bias value for an input.

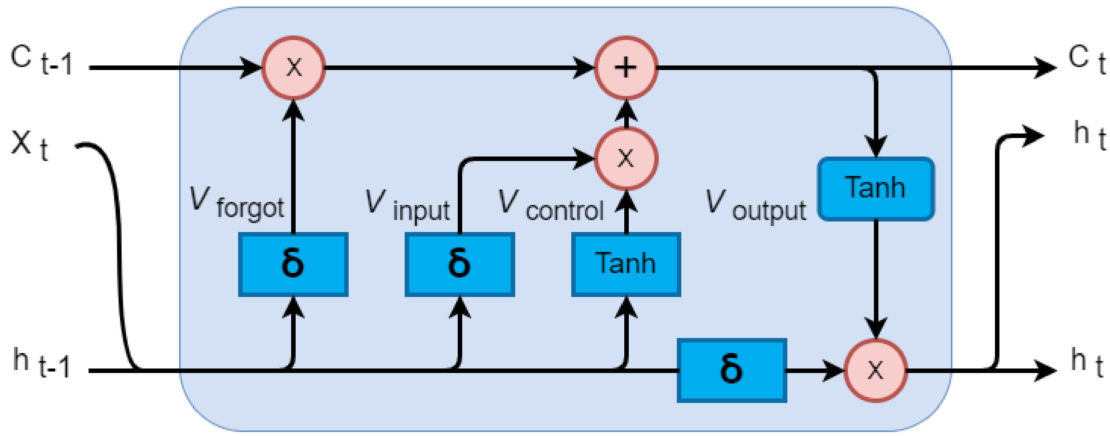

Fig. 2. *Proposed LSTM cell architectural scheme of the proposed study*

In Figure 2 LSTM network consists of three inputs. Where X_t is the input of the current time step. h_{t-1} is the output from the previous LSTM unit and the most important input C_{t-1} is the memory of the previous unit. While h_t and C_t are the output and memory of the current network.

4. Proposed Methodology

The proposed methodology is divided into several parts such as Data Formatting, Data Preprocessing, Modelling and Analysis which are illustrated in Figure 3.

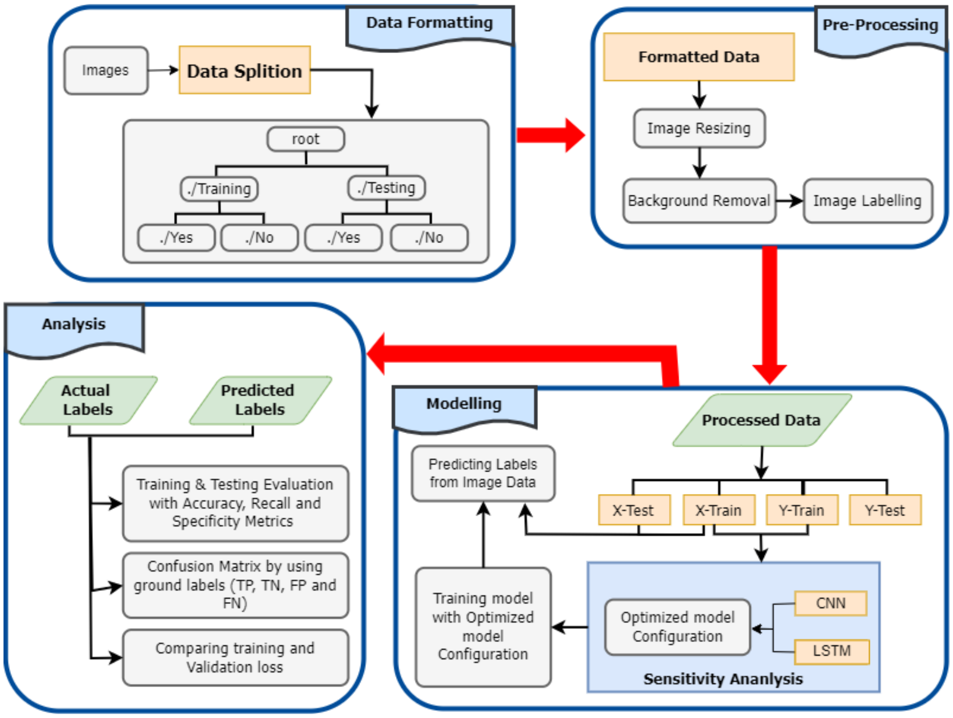

Fig. 3. *Graphical Scheme of Proposed Methodology*

a. Data Curation:

Data set implied in the study is collected from kaggle, which is an online database publicly available. Kaggle allows the user to explore different datasets, design and explore models in data science environment [31]. The data set is categorized into directories for training and testing data, which include labeled folders for "with tumor" and "without tumor" image data. To access the data through Google Colab, it is first uploaded onto Google Drive.

b. Data Preprocessing:

The data preprocessing is used to remove the noise data that is responsible for decrease in model's performance. Usually, MRI brain images are composed of surplus areas and spaces. The respective research uses the cropping technique in that uses the extreme point calculation [31]. The image dataset is also comprised of images with different sizes and shapes. Hence resizing the images in equal height and width is necessary for achieving the best possible outcome. The images were also resized to 128 by 128 pixels to standardize each image for the model input. Along with that, One Hot Encoding Technique was applied to each image which converts them into binary (0 and 1) format, to help the model better categorize the image into positive and negative tumor classes, respectively. The division of data into training and testing sets is achieved by a ratio of 90% and 10%, respectively.

c. Model Development:

The optimum classifier configuration for the given data set is necessary to increase accuracy and reduce errors. This configuration helps the model to better understand the data and best train itself according to the contrived data. In the proposed study, the optimized configuration was selected by trial-and-error technique. The models were executed with different combinations of model parameters and the most accurate one is taken for evaluation.

For CNN, the model has multiple layers which include Flatten, Maxpooling-2D, Conv2D, Dropout, Batch Normalization, and Dense layer. The detailed model summary is shown in table 2.

Table 2: *Model Summary for Convolution Neural Networks used in the respective study.*

Layers	Output Shape	Param #
Conv1	(None, 128, 128, 32)	416
Conv2	(None, 128, 128, 32)	4128
BN1	(None, 128, 128, 32)	128
Max1	(None, 64, 64, 32)	0
Drop1	(None, 64, 64, 32)	0
Conv3	(None, 64, 64, 64)	8256
Conv4	(None, 64, 64, 64)	16448
BN2	(None, 64, 64, 64)	256
Max2	(None, 32, 32, 64)	0
Drop2	(None, 32, 32, 64)	0
Flat1	(None, 65536)	0
Dense1	(None, 512)	33554944
Drop3	(None, 512)	0
Dense2	(None, 2)	1026
Total Params: 33,585,602		
Trainable Params: 33,585,410		
Non-trainable Params: 192		

Note: The Layers are represented as Conv2D (Conv), BatchNormalization (BN), MaxPooling2D (Max), Dropout (Drop), Flatten (Flat), Dense (Dense) in the table.

For LSTM, the model has also assembled by multiple layers which includes LSTM, Batch Normalization, Dropout and Dense Layer. The model summary is as follows in Table 3.

Table 3: *Model Summary for proposed LSTM Neural Networks for the study*

Layers	**Output Shape**	**Param #**
LSTM1	(None, None, 64)	12599552
LSTM2	(None, 64)	33024
BN1	(None, 64)	256
Dense1	(None, 512)	33280
Drop1	(None, 512)	0
Dense2	(None, 2)	1026
Total Params: 12,667,138		
Trainable Params: 12,667,010		
Non-trainable Params: 128		

Note: The Layers are represented as lstm (LSTM) BatchNormalization (BN), Dropout (Drop), Dense (Dense) in the table.

Both the models were optimized by an Adamax optimizer, and the loss function used was Categorical Cross entropy (CCE) represented in equation 8 [32]. Where, $E_{(k')}$ represents True label for K-th class while E_k represents output probability of K-th class vector.

$$CCE = -\sum E_{k'} . log\ (E_k) \qquad (8)$$

The activation function plays an important role in improving the performance of neural networks [33]. The Rectified Linear unit (ReLU) and softmax functions were selected for this classifier due to their promising results from past studies [33, 34]. The ReLU function works by threshold values at 0, as demonstrated in equation 9 [16].

$$f(x) = \begin{cases} x, for\ x > 0 \\ 0, for\ x \leq 0 \end{cases} \qquad (9)$$

The softmax function is used to specify a discrete probability distribution for K classes, as represented in equation 10 [34].

$$\sigma(x) = \frac{e^x}{\sum_{y=1}^{k} e^y} \qquad (10)$$

where, σ is represented as a softmax function, x is the input variable, while k represents the number of classes. e_x and e_y are the exponential function for the input and output variables, respectively.

5. Results and Discussion

5.1 Accuracy and Loss Graph:

For CNN, the accuracy and losses for training and validation data were determined at each epoch. The result for accuracy showed that the model should call back an early stopping as the validation accuracy began to decline after epoch=22, this might be due to over-fitting of the model. On the other hand, the training and validation losses exhibit a decrease until the model stabilizes, with losses becoming almost negligible at each epoch. This trend also supports the decision to implement early stopping, as it reduces computational space and time complexity. Figure 4(a1) & (b1) represents the accuracy and loss of training and validation data for CNN model, respectively.

For LSTM, the accuracy and losses for training and validation data was also determined for each epoch, similarly. The trend for accuracy graph depicts that the training and validation accuracy are slightly increasing or constant at epoch=15. On the other hand, the training losses tend to decline which indicates the early stopping as a suitable measure to reduce the risk of model being over-fitting. Figure 4(a2) & (b2) represent the accuracy and loss for both training and validation dataset for LSTM model, respectively.

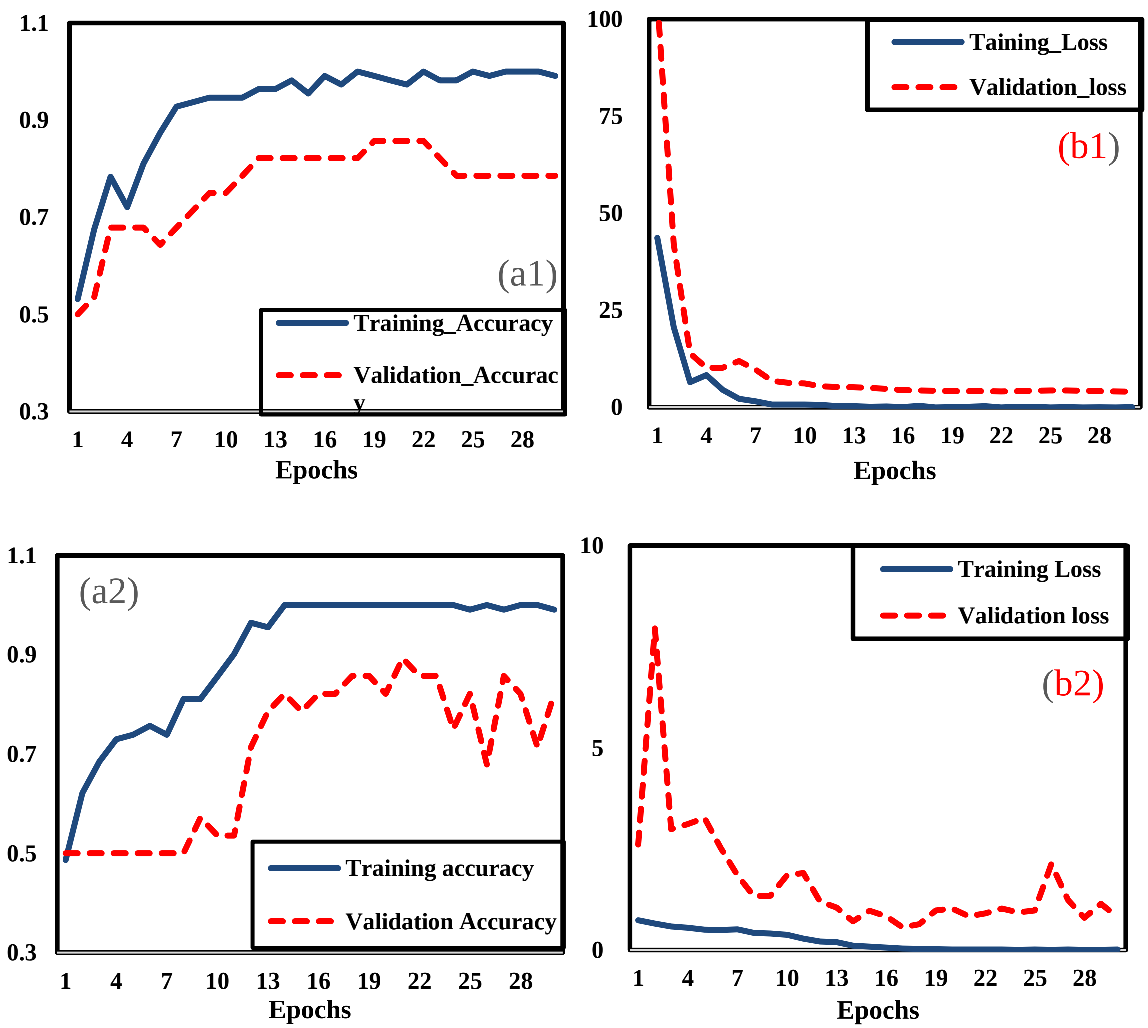

Fig. 4. Graphical Representation of training and validation (a1) & (b1) accuracy and loss for CNN, (a2) & (b2) accuracy and loss for LSTM model.

5.2 Confusion Matrix

A confusion matrix is a table that describes and depicts the efficiency of the classifying model [35]. It is also used to evaluate the performance of the classifier through different statistical metrics. The confusion matrix for CNN model of the respective study is presented in Figure 5. While for LSTM model the confusion matrix is as presented in Figure 6.

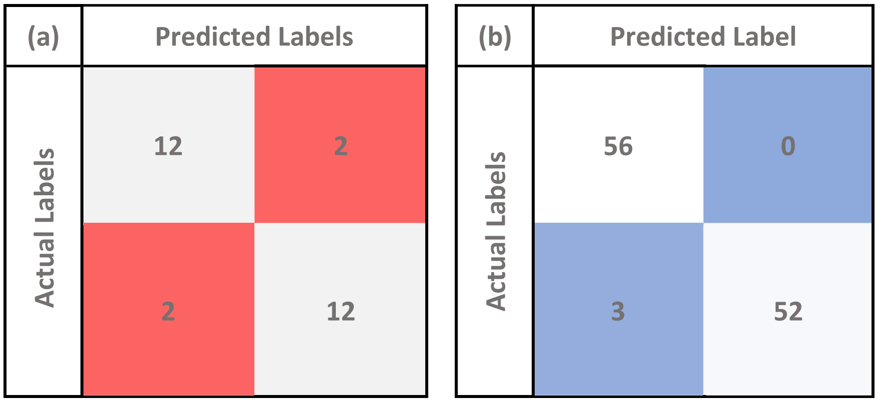

Fig. 5. *Graphical Scheme of Confusion Matrix for (a) training & (b) testing data of CNN model*

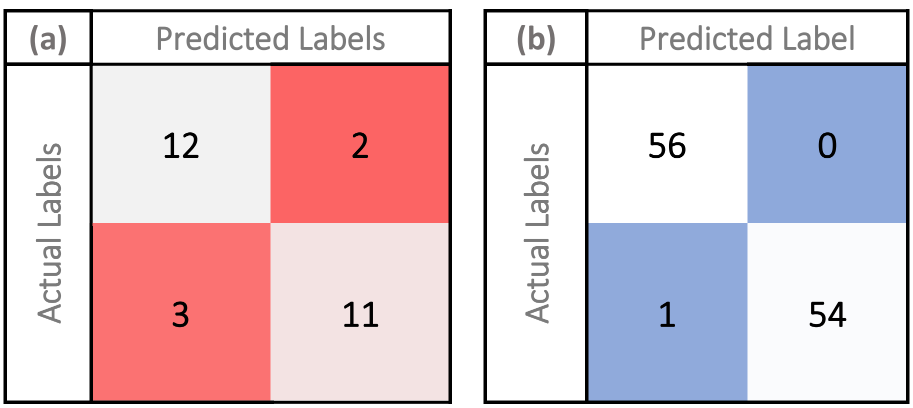

Fig. 6. *Graphical Scheme of Confusion Matrix for (a) training & (b) testing data of LSTM model*

In the respective study, the condition specifying that the classifier efficiently identifies a person with Tumor is known as True Positive (TP). While True negative is the condition in which the classifier accurately identifies a person with no tumor. Also, if the condition states a classifier inaccurately classifies a healthy person as having a tumor, then it is False Positive (FP). While if the classifier wrongly identifies a person with Tumor as a healthy person, then it is categorized as a False Negative (FN).

Statistically, Accuracy is the metric for measuring the proportionality of the classes that have been accurately classified. While the Recall metric is used to measure the proportionality of positive classes that have been classified correctly. Specificity metrics quantify the model's ability to accurately identify true negatives among the total negatives predicted, crucial for assessing the model's precision in ruling out non-tumor cases. While Misclassification (Error) Rate is a measure for finding the proportion of incorrectly classified classes [36]. The Evaluation for both the models for training and testing phase can be seen in Table 4.

Table 4: *Showing Statistical Evaluation of CNN & LSTM classifier through confusion matrix.*

Parameter	Formula	CNN		LSTM	
		Training (%)	Testing (%)	Training (%)	Testing (%)
Accuracy	$= ((\frac{(TP+TN)}{(TP+TN+FP+FN)}) * 100)\%$	97.3	85.71	98.22	92.86
Recall	$= ((\frac{(TP)}{(TP+TN)}) * 100)\%$	94.54	85.71	99.11	89.29
Specificity	$= ((\frac{(TN)}{(TN+FP)}) * 100)\%$	100	85.71	100	85.72
Misclassification Error	$= ((\frac{(FP+FN)}{(TP+TN+FP+FN)}) * 100)\%$	2.7	14.28	0.89	10.72

6. Conclusion

In this paper, a brain tumor classification technique is proposed while configuring the CNN and LSTM models with optimized Hyperparameter through trial-and-error technique. The model was selected due to their promising results in biomedical science. The preprocessed data was first used to train both models. The models were then observed and evaluated by different tests including validation and testing loss/accuracy graph, Confusion matrix and classification report. The results concluded that LSTM model have performed superior to CNN model in predicting Tumor images both on training dataset as well as on unseen data with accuracy of 98.22 and 92.86, respectively. While CNN model performs robustly in classifying tumor with an accuracy of 97.3 (on training data) and 85.71 (on testing data). Other metrics on testing data proves that LSTM (Recall: 89.29, Specificity: 85.72, Misclassification error: 10.72) outperformed CNN model (Recall: 85.71, Specificity: 85.71, Misclassification error: 14.28), implying that LSTM model is a suitable model for predicting tumor by MRI images while training on limited data.

The future work for this study could focus on utilizing the proposed algorithms in different medical sciences case studies, and scan images (like CT scan, etc.). The study can further extend to predict real-time brain-tumor using MRI-scanned videos which could include 3D imaging tumor detection which could be helpful in identifying different types of tumors.

Author Contribution

All Authors have contributed equally to the study.

Competing Interest

All Authors affirm that they have no competing interest for the study.

References

[1] Rebecca L. et al. "Cancer statistics, 2021," CA: a cancer journal for clinicians, **71**(1), 7–33 (2021).

[2] Akram, F. et al. Trustworthy intrusion detection in e-healthcare systems. Front. Public Health **9,** 788347. doi: 10.3389/fpubh.2021.788347 (2021).

[3] Houssein, E. H., Ibrahim, I. E., Hassaballah, M. & Wazery, Y. M. "Integration of internet of things and cloud computing for cardiac health recognition," in Metaheuristics in Machine Learning: Theory and Applications (Springer), 645–661 (2021).

[4] Zhang, L., Zhong, Q. & Yu, Z. (2021). Optimization of tumor disease monitoring in medical big data environment based on high-order simulated annealing neural network algorithm. Comput. Intell. Neurosci. 8996673. doi: 10.1155/2021/8996673 (2021).

[5] Kaur, T., Saini, B.S. & Gupta, S. "Quantitative metric formr brain tumour grade classification using sample space density measure of analytic intrinsic mode function representation," IET Image Processing, **11**(8), 620–632 (2017).

[6] Usman, K. & Rajpoot, K. "Brain tumor classification from multi-modality mri using wavelets and machine learning," Pattern Analysis and Applications, **20**(3), 871–881 (2017).

[7] Mohsen, H. et al. "Classification using deep learning neural networks for brain tumors," Future Computing and Informatics Journal, **3**(1), 68–71 (2018).

[8] Alanazi, M.F. et al. Brain tumor/mass classification framework using magnetic-resonance-imaging-based isolated and developed transfer deep-learning model. Sensors **22,** 372. doi: 10.3390/s22010372 (2022).

[9] Sultan, H.H., Salem, N.M. & Al-Atabany, W. "Multi-classification of brain tumor images using deep neural network," IEEE Access, **7,** 69215–69225 (2019).

[10] Edraki, M., Rahnavard, N. & Shah, M. "Subspace capsule network.," in AAAI, 10745–10753 (2020).

[11] Brain Tumor Detection Using Deep Neural Network and Machine Learning Algorithm by Masoumeh Siar; Mohammad Teshnehlab.

[12] Brain Tumor Detection Using Convolutional Neural Network by Tonmoy Hossain; Fairuz Shadmani Shishir.

[13] Lai, W., Hu, F., Kong, X., Yan, P., Bian, K. & Dai, X. "The study of coal gangue segmentation for location and shape predicts based on multispectral and improved Mask R-CNN," Powder Technol., **407,** 117655, Jul. 2022, doi: 10.1016/j.powtec.2022.117655 (2022).

[14] Ezhilarasi, R. & Varalakshmi, P. "Tumor Detection in the Brain using Faster R-CNN," in 2018 2nd International Conference on I-SMAC (IoT in Social, Mobile, Analytics and Cloud) (I-SMAC)I-SMAC (IoT in Social, Mobile, Analytics and Cloud) (I-SMAC), 2018 2nd International Conference on, Palladam, India: IEEE, Aug. 2018, 388–392. doi: 10.1109/I-SMAC.2018.8653705 (2018).

[15] Saeedi, S., Rezayi, S., Keshavarz, H. & Niakan Kalhori, S.R. "MRI-based brain tumor detection using convolutional deep learning methods and chosen machine learning techniques," BMC Med. Inform. Decis. Mak., **23**(1), 16, Jan. 2023, doi: 10.1186/s12911-023-02114-6 (2023).

[16] Shanthi, S., Saradha, S., Smitha, J.A., Prasath, N. & Anandakumar, H. "An efficient automatic brain tumor classification using optimized hybrid deep neural network," Int. J. Intell. Netw., **3,** 188–196, 20doi: 10.1016/j.ijin.2022.11.003 (2022).

[17] Kumar, D. M., Satyanarayana, D., & Prasad, M. Mri brain tumor detection using optimal possibilistic fuzzy c-means clustering algorithm and adaptive k-nearest neighbor classifier. J. Ambient. Intell. Humaniz Comput. **12,** 2867–2880. doi: 10.1007/s12652-020-02444-7 (2021).

[18] Zhou, H. et al. Automatic machine learning to differentiate pediatric posterior fossa tumors on routine mr imaging. Am. J. Neuroradiol. **41,** 1279–1285. doi: 10.3174/ajnr.A6621 (2020).

[19] Srikanth, B. & Venkata Suryanarayana, S. "WITHDRAWN: Multi-Class classification of brain tumor images using data augmentation with deep neural network," Mater. Today Proc., p. S2214785321006933, Mar. 2021, doi: 10.1016/j.matpr.2021.01.601.

[20] Asiri, A.A. et al., "Brain Tumor Detection and Classification Using Fine-Tuned CNN with ResNet50 and U-Net Model: A Study on TCGA-LGG and TCIA Dataset for MRI Applications," Life, **13**(7), 1449, Jun. 2023, doi: 10.3390/life13071449 (2023).

[21] Deepak, S. & Ameer, P.M. "Brain tumor classification using deep CNN features via transfer learning," Comput. Biol. Med., **111,** 103345, Aug. 2019, doi: 10.1016/j.compbiomed.2019.103345 (2019).

[22] Kesav, N. & Jibukumar, M.G. "Efficient and low complex architecture for detection and classification of Brain Tumor using RCNN with Two Channel CNN," J. King Saud Univ. - Comput. Inf. Sci., **34**(8), 6229–6242, Sep. 2022, doi: 10.1016/j.jksuci.2021.05.008 (2022).

[23] Alqudah, A.M. "Brain Tumor Classification Using Deep Learning Technique - A Comparison between Cropped, Uncropped, and Segmented Lesion Images with Different Sizes," Int. J. Adv. Trends Comput. Sci. Eng., **8**(6), 3684–3691, Dec. 2019, doi: 10.30534/ijatcse/2019/155862019 (2019).

[24] Khairandish, M.O., Sharma, M., Jain, V., Chatterjee, J.M. & Jhanjhi, N.Z. "A Hybrid CNN-SVM Threshold Segmentation Approach for Tumor Detection and Classification of MRI Brain Images," IRBM, **43**(4), 290–299, Aug. 2022, doi: 10.1016/j.irbm.2021.06.003 (2022).

[25] Öksüz, C., Urhan, O. & Güllü, M.K. "Brain tumor classification using the fused features extracted from expanded tumor region," Biomed. Signal Process. Control, **72,** 103356, Feb. 2022, doi: 10.1016/j.bspc.2021.103356 (2022).

[26] Tummala, S., Kadry, S., Bukhari, S.A.C. & Rauf, H.T. "Classification of Brain Tumor from Magnetic Resonance Imaging Using Vision Transformers Ensembling," Curr. Oncol., **29**(10), 7498–7511, Oct. 2022, doi: 10.3390/curroncol29100590 (2022).

[27] Kadry, S., Nam, Y., Rauf, H.T., Rajinikanth, V. & Lawal, I.A. "Automated Detection of Brain Abnormality using Deep-Learning-Scheme: A Study," in 2021 Seventh International conference on Bio Signals, Images, and Instrumentation (ICBSII), Chennai, India: IEEE, Mar. 2021, 1–5. doi: 10.1109/ICBSII51839.2021.9445122 (2021).

[28] Pareek M., Jha C.K. & Mukherjee S. Advances in Intelligent Systems and Computing. Springer; Singapore: 2020. Brain Tumor Classification from MRI Images and Calculation of Tumor Area, 73–83.

[29] Taye, M.M. "Theoretical Understanding of Convolutional Neural Network: Concepts, Architectures, Applications, Future Directions," Computation, **11**(3), 52, Mar. 2023, doi: 10.3390/computation11030052 (2023).

[30] Absar, N., Uddin, N., Khandaker, M. U. & Ullah, H. "The efficacy of deep learning based LSTM model in forecasting the outbreak of contagious diseases," Infect. DisModel., **7**(1), 170–183, Mar. 2022, doi: 10.1016/j.idm.2021.12.005 (2022).

[31] Dahiwade, D., Patle, G. & Meshram, E. "Designing disease prediction model using machine learning approach," in 2019 3rd International Conference on Computing Methodologies and Communication (ICCMC) (Erode: IEEE), 1211–1215 (2019).

[32] Gajowniczek, K., Liang, Y., Friedman, T., Ząbkowski, T. & Van den Broeck, G. "Semantic and Generalized Entropy Loss Functions for Semi-Supervised Deep Learning," Entropy, **22**(3), 334, Mar. 2020, doi: 10.3390/e22030334 (2020).

[33] Bai, Y. "RELU-Function and Derived Function Review," SHS Web Conf., **144,** 02006, doi: 10.1051/shsconf/202214402006 (2022).

[34] Agarap, A.F. "Deep Learning using Rectified Linear Units (ReLU)," Mar. 2018.

[35] Singh, P., Singh, N., Singh, K.K. & Singh, A. "Diagnosing of disease using machine learning," in Machine Learning and the Internet of Medical Things in Healthcare, Elsevier, 89–111. doi: 10.1016/B978-0-12-821229-5.00003-3 (2021).

[36] Upadhyay, N.A., Lalwaney, A. & Sharma, A. “Pancreatic Cancer Detection Using Radial Basis Neural Network,” SN Comput. Sci., **4**(3), 261, Mar. 2023, doi: 10.1007/s42979-022-01643-7 (2023).